APL Electronic Devices ARTICLE pubs.aip.org/aip/aed

Controlled size Ag nanoparticle doped CSA-PANI composite for efficient ultraviolet photodetection

Cite as: APL Electron. Devices 1, 046112 (2025); doi: 10.1063/5.0295954
Submitted: 12 August 2025 • Accepted: 10 October 2025 •
Published Online: 22 October 2025

Shivani Sharma,[1] Rishibrind Kumar Upadhyay,[1,a)] Dipika Sharma,[2] and Satinder K. Sharma[3,b)]

AFFILIATIONS

[1] Department of Electronics and Communication Engineering, Jaypee Institute of Information Technology, Noida-62, Uttar Pradesh 201309, India
[2] Department of Chemistry, Indian Institute of Technology Delhi, New Delhi 110016, India
[3] School of Computing and Electrical Engineering, Indian Institute of Technology Mandi, Himachal Pradesh 175005, India

[a)] **Author to whom correspondence should be addressed:** rishibrind.upadhyay@jiit.ac.in
[b)] **Email:** satinder@iitmandi.ac.in

ABSTRACT

We report the enhanced ultraviolet (UV) photodetection performance of a size-controlled silver nanoparticle (Ag NP) doped camphorsulfonic acid (CSA) doped polyaniline (PANI) composite with a cost effective approach. The uniform dispersion and controlled size (~5 nm) of Ag NPs within the CSA-PANI matrix are prepared by using the water-in-oil microemulsion technique and chemical sol-gel route. The surface morphology of prepared Ag nanoparticles doped CSA-PANI has been examined by transmission electron microscopy (TEM). The integration of Ag NPs to CSA-PANI contributes to increased carrier mobility and conductivity of the samples. The optoelectronics properties of the fabricated photodetector have been examined using a semiconductor parametric analyzer for biased voltages of −1 to 1 V. A rise time of ~2.7 ms and a fall time of ~1.9 ms have been observed with the proposed device. The synergistic effect of Ag size control and conductive polymer offers a promising path for scalable, low-cost UV photodetectors in optoelectronic applications.

I. INTRODUCTION

Conducting polymers have received attention as promising materials in the realm of optoelectronic devices owing to their versatile structural variations, electrochemical attributes, and electrical properties. Their ability to be processed easily from solutions enhances their appeal, offering a straightforward fabrication process at a low cost.[1–4] CSA-doped Polyaniline (CSA-PANI), belonging to the conducting polymer group, demonstrates promising attributes as a p-type semiconductor.[5] It exhibits notable characteristics, such as excellent chemical stability, significant electrical conductivity, robust environmental resilience, and cost-effective processing capabilities.[6] It is extensively used in optoelectronic and electronic applications, switches, batteries, etc.[7–10] Furthermore, research indicates that CSA-PANI synthesized utilizing m-cresol as a solvent displays enhanced electrical conductivity attributed to the development of expanded coil structures.[11]

Research on PANI-based nanocomposite has been thorough, focusing on applications, such as dopamine detection,[12] microbial fuel cells,[13] photo-detection,[14] chemical sensors,[15] and biosensors.[16] It is worth noting that while there is substantial literature on these applications, there is relatively limited documentation on the photo-detection capability of polyaniline metal nanoparticle nanocomposite.[17–19]

Metallic nanoparticles exhibit strong light absorption and scattering properties due to surface plasmon (SP) resonances. These SPs are collective oscillations of conduction electrons at the nanoparticle surface, triggered by incident light. According to classical electrodynamics, they appear as evanescent surface waves. On account of their exhibit strong light absorption and scattering properties metallic nanoparticles with a controlled size are promising catalyst for photodetection applications. Numerous studies support the presence of SPs for gold and silver nanoparticles under the visible spectral region[20–22] and near UV spectral region.[23] However, there are few

reports on silver and gold nanoparticles, showing the SPR effect in the UV-C region.

Nanocomposite material comprising silver nanoparticles [Ag (NPs)] embedded within a matrix of polyaniline (PANI) and camphorsulfonic acid (CSA) is synthesized using a water-in-oil emulsion technique, next to this, the polymerization of aniline in the presence of Ag (NPs). Subsequently, UV detection application is explored. To evaluate its performance, the nanocomposite thin films are drop casted onto a micro-interdigitated electrode (μ-IDE) structure based on aluminum. The μ-IDE structure is chosen for its ability to mitigate the resistance associated with organic compounds. By reducing resistance, the μ-IDE structure enhances the sensitivity of the device, thereby improving its capability to detect ultraviolet radiation.[18,24]

Herein, we explored the synthesis of controlled size ~5 nm Ag nanoparticles and its doping effect to CSA-PANI nanocomposite thin-film as UV light photodetector. We have prepared the controlled size ~5 nm Ag nanoparticles using a cost effective approach of water-in-oil emulsion technique, and for the fabrication of nanocomposite, simple chemical sol-gel route has been adopted. The morphological characters, such as shape and size of the prepared Ag nanoparticles doped CSA-PANI, have been determined by transmission electron microscopy (TEM). The optoelectronics properties of the fabricated photodetector have been examined using a semiconductor parametric analyzer for biased voltages of −1 to 1 V. The fabricated device displays a rise time of ~2.7 ms and a fall time of ~1.9 ms.

II. EXPERIMENTAL

A. Materials and synthesis

The monomer aniline, sourced from Fisher scientific with a purity of 99%, is employed in polymerization process, alongside the oxidant ammonium peroxydisulphate (APS) with a purity of 98%, and hydrochloric acid (HCl). Merck provides m-cresol as the solvent, ensuring a purity level of 99.5%. In the synthesis of Ag (NPs) using the water-in-oil microemulsion technique, Fisher scientific supplies the metal salt $AgNO_3$, while Sigma-Aldrich offers the surfactant dioctyl sulfosuccinate sodium salt (AOT), the oil toluene, and the reducing agent hydrazine hydrate.

A precise synthesis protocol was followed to prepare the nanoparticles. Sub-5 nm silver nanoparticles were synthesized using specific concentrations of chemicals: 0.02M of $AgNO_3$ salt, AOT (0.005M) as the surfactant, and reducing agent of hydrazine hydrate (0.2M). Initially, 100 μl of surfactant was added dropwise to 2 ml of silver salt solution (0.02M) under continuous stirring at 800 rpm for 5 min using a magnetic stirrer. Next, 8 ml of toluene was added to the mixture, and stirring was continued for another 10 min at the same speed. Subsequently, 0.2 ml of the reducing agent was introduced dropwise to initiate the reduction of Ag^{2+} ions into silver nanoparticles as illustrated in Fig. 1. The reaction mixture was then stirred continuously for 10 h at 800 rpm to achieve the desired nanoparticle size.

The nanocomposite was synthesized by incorporating silver nanoparticles during the chemical polymerization of the monomer, resulting in their encapsulation within the polymer matrix. The Ag (NPs)/CSA-PANI nanocomposite was prepared via oxidative polymerization at a controlled temperature of ~0–5 °C. Initially, 0.2M aniline monomer was dissolved in 100 ml of 1M HCl at 0 °C. Then, 1 ml of the nanoparticle solution in toluene was added, and the mixture was stirred for 15 min. Following this, 33 ml of 0.8M ammonium peroxydisulfate $[(NH_4)_2S_2O_8]$ was added dropwise to the solution under continuous stirring. The reaction was allowed to proceed for 4 h at around 0 °C until the solution turned green, indicating successful polymerization.[7] This process ensured the formation of the desired molecular weight of the polymer, as illustrated in Fig. 2. The synthesized solution was left for ~8 h at ~0 °C to allow the settling of the resulting polymerized Ag (NPs)/CSA-PANI precipitates, followed by rinsing with acetone and then DI water to remove the aniline oligomers. Subsequently, the precipitates were vacuum dried at 60 °C for 12 h to obtain emeraldine Ag (NPs)/CSA-PANI powder. Following this, Ag (NPs)/CSA-PANI and camphorsulfoic acid (0.2 ml) were mixed with m-cresol in a ratio of 1:10. Later, the

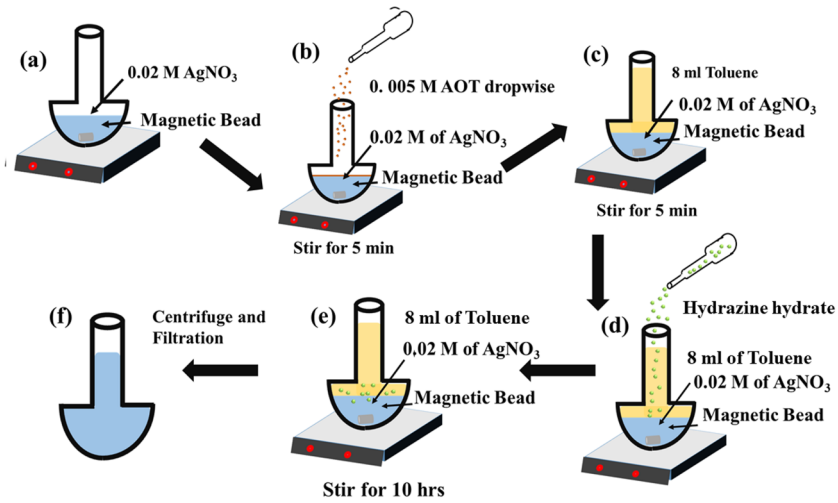

FIG. 1. Synthesis flow of Ag nanoparticles (Ag NPs) using the water-in-oil microemulsion method: (a) preparation of 0.02M silver nitrate solution, (b) addition of 0.005M AOT surfactant to generate micelles for trapping Ag^+ ions, (c) addition of 8 ml toluene as the organic phase, (d) reduction using hydrazine hydrate, (e) continuous stirring for 10 h to achieve the desired nanoparticle size, and (f) centrifugation and filtration to separate smaller-sized Ag NPs.

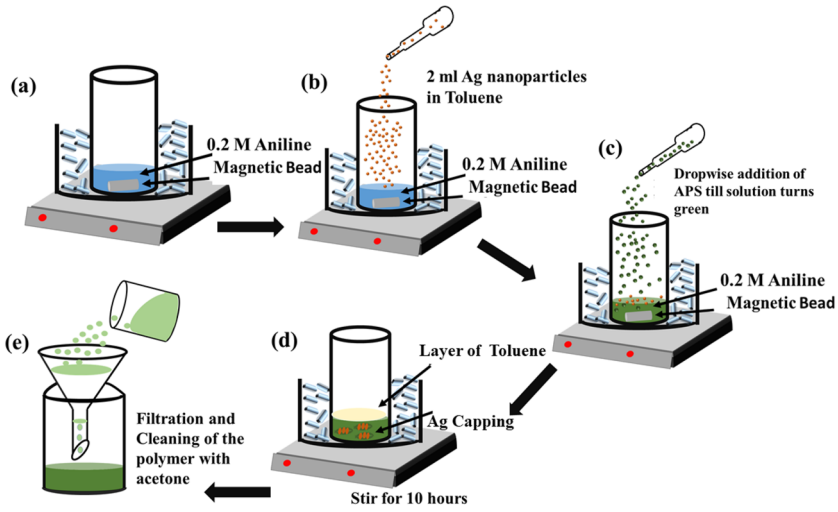

FIG. 2. Ag (NP)/CSA-PANI nanocomposite synthesis process: (a) 0.2M aniline solution maintained at 0 °C using an ice bath, (b) incorporation of Ag nanoparticles into the aniline matrix to enable embedding within PANI fibers, (c) addition of APS as an oxidant to initiate polymerization, (d) continuous stirring for 10 h to achieve the desired polymerization length, and (e) filtration and drying to obtain the Ag NP/CSA-PANI nanocomposite.

solution was stirred at 60 °C for 2 h, followed by ultrasonic treatment for 15 min to obtain a homogeneous Ag (NP)/CSA-PANI nanocomposite solution.

B. Device fabrication

The glass slides sourced from Bluestar underwent a thorough cleaning process involving several steps. Initially, they were subjected to sonication in a soapy solution for 10 min, followed by a similar treatment in deionized (DI) water for another 10 min. Next, they were boiled in acetone for 10 min at 60 °C and then sonicated in IPA (isopropyl alcohol) for an additional 10 min. The cleaning process concluded with drying using N_2 gas and baked at 200 °C for 15 min for dehydration. Following cleaning, the dummy substrate was cooled down to room temperature (RT). Subsequently, a thin film of Al (~100 nm) was deposited onto the glass samples using a thermal evaporator under ultrahigh vacuum of ~1.0×10^{-6} mbar. The 17 fingers of μIDE structure were fabricated with the width (W) = gap (D) = 300 μm, length (L) = 0.2 cm, as reported elsewhere.[24]

Finally, the Ag (NP)/CSA-PANI nanocomposite was spin-coated over the Al μ-IDE electrode, as indicated in Fig. 3(d).

III. RESULTS AND DISCUSSION

A. Material characterization

Figures 4(a) and 4(b) display the HR-TEM images of the as synthesized Ag (NPs) and the Ag (NP)/CSA-PANI nanocomposite images were taken using high resolution transmission electron microscopy (Tecnai G 2 20 S-TWIN), respectively. It has been observed that Ag (NPs) with a typical particle size of about 1.5–5 nm are uniformly distributed. The uniform distribution and controlled size of Ag (NPs) can be attributed to a cost-effective, single-step synthesis approach, where the concentrations of both the surfactant and the reducing agent were carefully optimized and minimized. This simplified method not only reduces material and processing costs but also offers scalability, opening avenues for broader applications of the nanocomposite in areas such as sensing and photocatalysis.

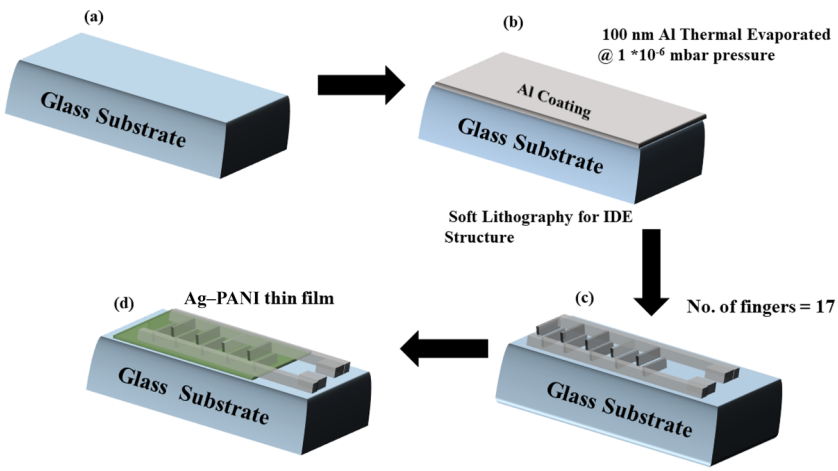

FIG. 3. Schematic diagram of Ag (NP)/CSA-PANI/Al μ-IDE MSM structure: (a) cleaning of the glass substrate, (b) thermal deposition of Al for electrode formation followed by photolithography to obtain the desired Al pattern, (c) completed electrode structure with 17 fingers to ensure maximum utilization of the active film in subsequent steps, and (d) spin-coating of the Ag NP/CSA-PANI film using m-cresol as a solvent.

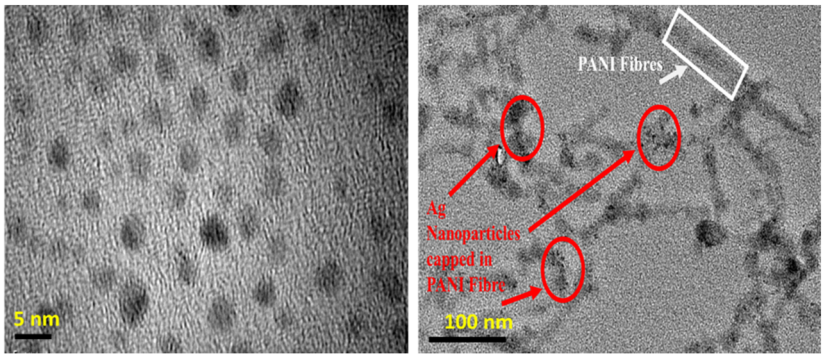

FIG. 4. HR-TEM images: (a) Ag (NPs) nanoparticles and (b) Ag (NP)/CSA-PANI nanocomposite.

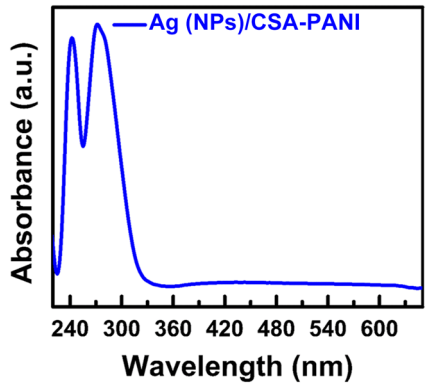

FIG. 5. UV–Vis absorption spectra of Ag (NP)/CSA-PANI nanocomposite.

Figure 5 shows the UV–Vis absorption spectra of the prepared Ag (NP)/CSA-PANI nanocomposite. It is clearly evident that the sub-5 nm Ag nanoparticles and CSA-PANI exhibit strong absorption below 300 nm, confirming that the device is active in the UV-C region, as further supported by the I–V characteristics.

B. Device characterizations

1. Electrical characterization

The current density–voltage (J–V) characteristics of an Ag (NP)/CSA-PANI based proposed device measured by a parameter analyzer (from the Keithley 4200 SCS) are shown in Fig. 6 over −1–1 V. J–V characteristics were measured under illumination of a UV light source with wavelength 254 nm and power 300 μW/cm^2 at room temperature (27 °C). Notably, Fig. 6 highlights a significant difference in both forward and reverse currents under UV illumination, on account of the photogenerated charge carriers, Consequently, the Al/Ag (NP)/CSA-PANI/Al structure exhibits photodetector traits, demonstrating a contrast ratio [the ratio of photocurrent (I_{ph}) to dark current (I_d)] of ~2.65 × 10^3 at −1 V. The higher contrast ratio of 2.65 × 10^3 Al/Ag (NP)/CSA-PANI/Al based proposed MSM structure strengthens its latent candidature as a competent UV-C photodetector.

The responsivity (R_{UV}), photoconductive gain (g), sensitivity (S), and detectivity (D) of the Al/Ag (NPs)/CSA-PANI/Al device computed using the following equations:[25–30]

$$R_{UV} = \frac{I_{PH}}{P_{OPT}}, \tag{1}$$

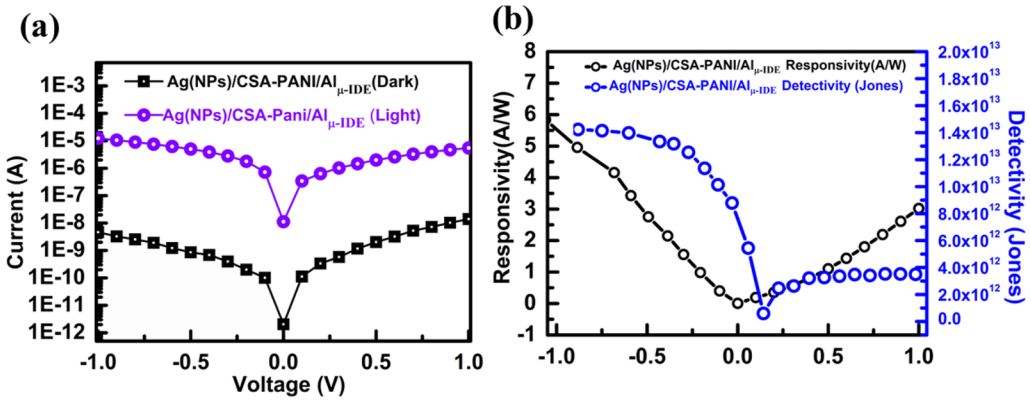

FIG. 6. (a) Semi-log current density voltage (J–V) characteristics of the Al/Ag (NP)/CSA-PANI/Al based photodetector under dark and illumination of light. (b) Responsivity and detectivity of the Al/Ag (NP)/CSA-PANI/Al, based photodetector.

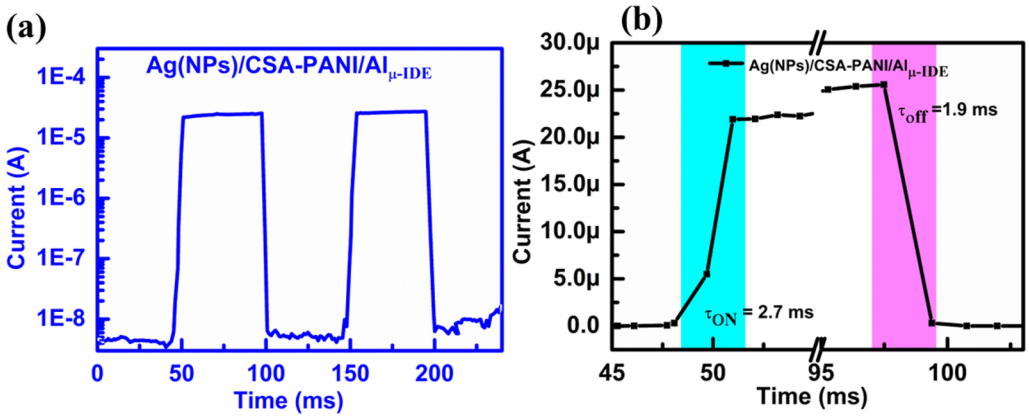

FIG. 7. Current–time (*I*–*t*) characteristics of (a) Al/Ag (NP)/CSA-PANI/Al device and (b) rise time and fall time for Al/Ag (NP)/CSA-PANI/Al device at −1 V bias.

$$g = \frac{1240 \times R_{UV}}{\lambda(\text{nm}) \times \eta}, \tag{2}$$

$$S = \left(\frac{I_{illum} - I_{dark}}{I_{dark}}\right) \times 100, \tag{3}$$

$$D = \frac{R_{UV}\sqrt{A}}{\sqrt{2 * q * I_{dark}}}), \tag{4}$$

where I_{PH}, P_{OPT}, and λ (nm) are the photocurrent at −1 V, the optical power, and the wavelength (in nm) of the incident UV light, respectively. Using Eqs. (1) and (2), we obtained much higher value parameter responsivity (R_{UV}) ~5.836 A/W, photoconductive gain (g) ~28.49, sensitivity ~2.66×10^5, and detectivity 1.41×10^{13} Jones for the Al/Ag (NP)/CSA-PANI/Al device.

The MSM photodetector structure was biased at −1 V to evaluate its maximum response under UV illumination (wavelength: 254 nm, intensity: 300 μW/cm^2). The current was monitored by periodically switching the UV light ON and OFF at intervals of ~50 ms. In this context, the rise time and fall time are defined as the durations required for the current to increase from 10% to 90% and decrease from 90% to 10% of its maximum value.[7,18] As shown in Fig. 7, the Al/Ag (NP)/CSA-PANI/Al device exhibited a rise time of ~2.7 ms and a fall time of around 1.9 ms. Furthermore, the performance of the state-of-art UV-C photodetectors as reported in the literature is summarized in Table I.

The mechanistic aspects of the proposed fabricated device have been demonstrated using the energy level position as shown in Fig. 8. Figure 8(a) depicts the proposed operational model of the device, schematically outlining the Al/Ag (NP)/CSA-PANI/Al MSM structure. In Fig. 8(a), a corresponding band diagram illustrates the configuration of the Ag (NPs) in the polyaniline fibers. In organic semiconductors, the conductivity of the material is strongly modulated by incident light. The incorporation of the Ag nanoparticles into a PANI matrix has been widely reported to enhance the optoelectronic properties through a combination of plasmonic effects and efficient charge transfer. The Ag nanoparticles introduce localized surface plasmon resonance (LSPR), which amplifies the local electromagnetic field and increases light absorption within the PANI backbone.[37–39] The incorporation of highly sensitive Ag (NPs) within CSA-PANI creates a conduction path to the μ-IDE, functioning as nanoelectrodes, which increase the overall conductivity of the device.[18,40] These findings are further supported by studies on Ag–graphene oxide–PANI hybrids, which showed that the Ag nanoparticles can strongly interact with the nitrogen sites in PANI, mediating fast electron transfer processes.[41] When the composite is exposed to UV light at a wavelength of 254 nm, surface

TABLE I. Benchmarking against the state-of-the-art MSM UV-C photodetectors.

S.No.	Materials	Bias (V)	Responsivity	Detectivity	Rise/Fall time	References
1	Pentacene	4	3.37 A/W	5.59×10^8 Jones	⋯	31
2	AlYN	−2	35.7 μA/W	1.42×10^{10} Jones	⋯	32
3	$MAPbI_3$	4	12×10^3 mA/W	0.1×10^{12} Jones	2.2/4 ms	33
4	$CsPbBr_3$	2	0.24 mA/W	1.9×10^{10}	0.26/0.28 s	34
5	β-Ga_2O_3	0	11.6×10^{-3} mA/W	⋯	1.78/33.06 s	35
6	WS_2-PANI	0	17.26 mA/W	2.08×10^{13} Jones	1.3/1.2 s	36
7	Ag (NPs)/CSA-PANI	−1	~5.836 A/W	1.41×10^{13} Jones	2.7/1.9 ms	This work

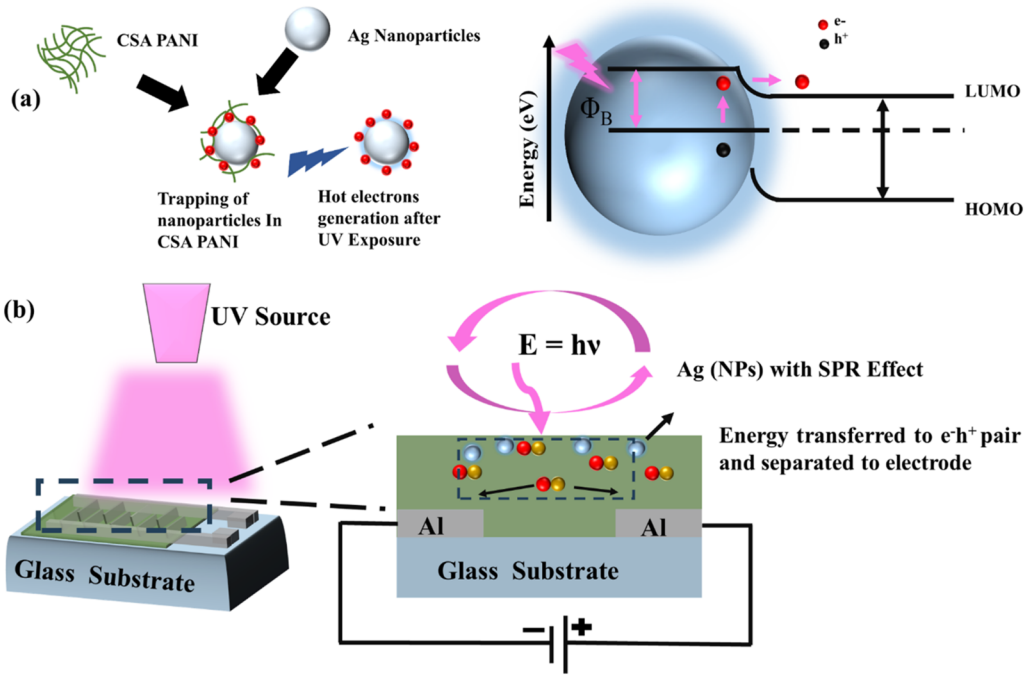

FIG. 8. Schematic for the charge transfer process from Ag (NPs) to the LUMO of the CSA-PANI during SPR effect. (b) Electron–hole pair generation in Al/Ag (NPs)/CSA-PANI/Al with applied bias and UV exposure.

plasmonics are induced on the Ag (NPs).[42–44] These surface plasmons facilitate the generation of electron–hole pairs in the conduction band of the metal through the decay of surface plasmonics.[45,46] The excited (hot) electrons then populate normally vacant states in the metal's conduction band before transferring to the polymer's lowest unoccupied molecular orbital (LUMO) [as depicted in Fig. 8(a)]. As a result, the current flowing through the device under illumination with light,[18,21,47,48] matching the localized surface plasmon resonance frequency, is significantly enhanced compared to the dark condition. The photogenerated charge carriers contributing to the current are collected at the surface of the electrode as the diffusion length in polymers is typically less than 10 nm. To maximize the utilization of generated charge carriers, the electrode geometry plays a crucial role.

IV. CONCLUSION

This article presents the development and characterization of a UV photodetector based on a solution-processed Al/Ag(NP)/CSA-PANI/Al structure. A key feature of this work is the use of a simple, solution-based synthesis route for the preparation of controlled-size silver nanoparticles (Ag NPs), which were then embedded in a CSA-doped polyaniline (PANI) matrix. This approach ensured uniform particle size distribution and effective dispersion within the polymer matrix. The device demonstrates excellent performance under ultraviolet (UV) illumination, particularly at a wavelength of 254 nm and a power intensity of 300 μW/cm^2. The photodetector exhibits a high responsivity of ~5.836 A/W, along with a remarkable sensitivity (S) of ~2.66×10^5 and detectivity (D) of ~1.41×10^{13} Jones. These values reflect the efficient photogeneration and transport of charge carriers within the composite structure. The device under a reverse bias of −1 V showed an encouraging response speed with a reasonably low rise time of ~2.7 ms and fall time of ~1.9 ms. These response characteristics indicate good temporal resolution and switching behavior, essential for practical photodetector applications.

ACKNOWLEDGMENTS

The authors would like to acknowledge the *Center for Design and Fabrication of Electronic Devices (C4DFED)*, Indian Institute of Technology (IIT), Mandi, (H.P), India, for the fabrication and characterization facilities.

AUTHOR DECLARATIONS

Conflict of Interest

The authors have no conflicts to disclose.

Author Contributions

Shivani Sharma: Conceptualization (equal); Data curation (equal); Formal analysis (equal); Investigation (equal); Methodology (equal); Project administration (equal); Validation (equal); Visualization (equal); Writing – original draft (equal); Writing – review &

editing (equal). **Rishibrind Kumar Upadhyay**: Conceptualization (equal); Data curation (equal); Investigation (equal); Methodology (equal); Resources (equal); Validation (equal); Visualization (equal); Writing – original draft (equal); Writing – review & editing (equal). **Dipika Sharma**: Writing – original draft (equal); Writing – review & editing (equal). **Satinder K. Sharma**: Conceptualization (equal); Formal analysis (equal); Investigation (equal); Methodology (equal); Project administration (equal); Resources (equal); Supervision (equal); Writing – original draft (equal).

DATA AVAILABILITY

The data that support the findings of this study are available from the corresponding author upon reasonable request.

REFERENCES

[1] O. B. Okafor, A. P. I. Popoola, O. M. Popoola, and S. O. Adeosun, Next Mater. **6**, 100389 (2025).
[2] S. Ameen, M. Song, D. G. Kim, Y.-B. Im, H. K. Seo, Y. S. Kim, and H. S. Shin, Macromol. Res. **20**, 30 (2012).
[3] S. Liao, C. Wang, H. He, and Y. Fu, Opt. Mater. **163**, 117032 (2025).
[4] P. K. Mishra, H. K. Sharma, R. Gupta, M. Manglik, and R. Brajpuriya, Microchem. J. **208**, 112369 (2025).
[5] B. T. Raut, M. A. Chougule, S. R. Nalage, D. S. Dalavi, S. Mali, P. S. Patil, and V. B. Patil, Ceram. Int. **38**, 5501 (2012).
[6] S. Ozbay, I. Korkut, and F. Erden, Colloids Surf. A **667**, 131381 (2023).
[7] S. Sharma, R. Khosla, D. Deva, H. Shrimali, and S. K. Sharma, Sens. Actuators A **261**, 94 (2017).
[8] S. Mridha and D. Basak, Appl. Phys. Lett. **92**, 142111 (2008).
[9] Z. Liu, J. Zhou, H. Xue, L. Shen, H. Zang, and W. Chen, Synth. Met. **156**, 721 (2006).
[10] K. Mahmood, K. Khalid, U. Amara, M. Z. U. R. Faurooqi, M. Ramzan, M. Hanif, H. M. Asif, J. Iqbal, F. Rasheed, F. Siddique, and Z. P. Liu, Int. J. Hydrogen Energy **119**, 126 (2025).
[11] X. Feng, C. Mao, G. Yang, W. Hou, and J. J. Zhu, Langmuir **22**, 4384 (2006).
[12] A. Tejwani, U. Sonkar, K. Shrivas, K. Tandey, I. Karbhal, M. K. Deb, and S. Pervez, RSC Adv. **15**, 15870 (2025).
[13] J. Ahmed and S. Kim, RSC Adv. **14**, 34498 (2024).
[14] H. Khudeir, K. A. Hubeatir, and F. A. Umran, J. Opt. **53**, 4834 (2024).
[15] A. S. Conejo-Dávila, A. Vega-Rios, A. Domínguez-Aragón, E. Aparicio-Martínez, R. B. Dominguez, and E. Armando Zaragoza-Contreras, "Recent advances in applications of polyaniline copolymers for chemical sensors with enhanced performance," in *Advanced Polymers*, edited by S. J. Ikhmayies (Springer Nature Switzerland, Cham, 2024), pp. 225–270.
[16] Y.-H. Chiu, M. Rinawati, L.-Y. Chang, Y.-T. Guo, K.-J. Chen, H.-C. Chiu, Z.-H. Lin, W.-H. Huang, S.-C. Haw, and M.-H. Yeh, ACS Appl. Nano Mater. **8**, 2340 (2025).
[17] P. Kumar, S. Suhag, J. R. Mandal, and V. K. Shahi, J. Membr. Sci. **711**, 123168 (2024).
[18] S. Sharma, S. Das, R. Khosla, H. Shrimali, and S. K. Sharma, J. Mater. Sci. Mater. Electron. **30**, 7534–7542 (2019).
[19] S.-W. Lee, J.-S. Lee, H.-W. Yu, T.-H. Kim, and H.-S. Kim, Polymers **17**, 1825 (2025).
[20] D. Geng and H. Y. Yang, Adv. Mater. **30**, 1800865 (2018).
[21] T. Barman and A. R. Pal, ACS Appl. Mater. Interfaces **7**, 2166 (2015).
[22] I. Tanabe, Anal. Sci. **41**, 1213 (2025).
[23] Y. Liu, X. Zhang, J. Su, H. Li, Q. Zhang, and Y. Gao, Opt. Express **22**, 30148 (2014).
[24] S. Sharma, R. K. Upadhyay, N. S. Babu, and S. K. Sharma, J. Alloys Compd. **1001**, 175096 (2024).
[25] J. Zheng, X. Ma, X. He, M. Gao, and G. Li, Procedia Eng. **27**, 1478 (2012).
[26] R. K. Upadhyay, A. P. Singh, D. Upadhyay, D. K. Jarwal, C. Kumar, and S. Jit, IEEE Electron Device Lett. **41**, 1225 (2020).
[27] M. El-Ghobashy, H. Hashim, M. Darwish, M. Khandaker, A. Sulieman, N. Tamam, S. Trukhanov, A. Trukhanov, and M. Salem, Nanomaterials **12**, 1103 (2022).
[28] A. Kathirvel, A. Uma Maheswari, and M. Sivakumar, Thin Solid Films **761**, 139534 (2022).
[29] L. Sang, M. Liao, and M. Sumiya, Sensors **13**, 10482 (2013).
[30] A. Ansari, S. Ahmed, M. H. J. Mashniwi, S. M. Shinde, A. Khan, P. Ranjan, and D. S. Negi, J. Mater. Sci. **60**, 2711 (2025).
[31] K. A. Hussain, G. M. Ali, A. Boubaker, and A. Kalboussi, J. Electron. Mater. **53**, 918 (2024).
[32] X. Jiang, Y. Wu, J. Qi, Y. Liu, Y. Wang, B. Zhou, S. Yu, and X. Zhou, IEEE Sens. J. **24**, 25581 (2024).
[33] W. Zheng, R. Lin, Z. Zhang, Q. Liao, J. Liu, and F. Huang, Nanoscale **9**, 12718 (2017).
[34] T. Zhang, F. Wang, P. Zhang, Y. Wang, H. Chen, J. Li, J. Wu, L. Chen, Z. D. Chen, and S. Li, Nanoscale **11**, 2871 (2019).
[35] B. R. Tak, M.-M. Yang, Y.-H. Lai, Y.-H. Chu, M. Alexe, and R. Singh, Sci. Rep. **10**, 16098 (2020).
[36] A. Singh and P. Chauhan, ACS Appl. Opt. Mater. **2**, 28 (2024).
[37] H. A. Ghaly, A. S. El-Kalliny, T. A. Gad-Allah, N. E. A. Abd El-Sattar, and E. R. Souaya, RSC Adv. **7**, 12726 (2017).
[38] W. N. Benahmed, I. Bekri-Abbes, and E. Srasra, J. Spectrosc. **2018**, 7320654 (2018).
[39] Q. M. Al-Bataineh, M. Telfah, R. Abu-Zurayk, A. Benchaabane, C. J. Tavares, and A. Telfah, Mater. Chem. Phys. **293**, 126816 (2023).
[40] M. Soni, T. Arora, R. Khosla, P. Kumar, A. Soni, and S. K. Sharma, IEEE Sens. J. **16**, 1524 (2016).
[41] V. Kumar, R. K. Gupta, R. K. Gundampati, D. K. Singh, S. Mohan, S. H. Hasan, and M. Malviya, RSC Adv. **8**, 619 (2018). H.-J. Liu, Z.-C. Chen, Y.-C. Chang, and C.-Y. Wu, Sens. Actuators A **379**, 115923 (2024).
[42] A. M. Alharbi, N. M. Ahmed, A. Abdul Rahman, N. Zahirah Noor Azman, S. Algburi, I. A. Wadi, A. M. Binzowaimil, O. Aldaghri, and K. H. Ibnaouf, Photonics Nanostruct.-Fundam. Appl. **58**, 101228 (2024).
[43] M. N. S. M. Ismail, M. A. S. A. Fahri, C. L. Tan, and R. Zakaria, Sci. Rep. **15**, 6 (2025).
[44] H.-J. Liu, Z.-C. Chen, Y.-C. Chang, and C.-Y. Wu, Sens. Actuators A **379**, 115923 (2024).
[45] K.-C. Lee, S.-J. Lin, C.-H. Lin, C.-S. Tsai, and Y.-J. Lu, Surf. Coat. Technol. **202**, 5339 (2008).
[46] G. N. Abdelrasoul, F. Pignatelli, I. Liakos, R. Cingolani, and A. Athanassiou, Composites, Part B **149**, 178 (2018).
[47] K. Kaarthik, C. Vivek, and B. Balraj, J. Photochem. Photobiol. A: Chem. **452**, 115480 (2024).
[48] S. Mubeen, G. Hernandez-Sosa, D. Moses, J. Lee, and M. Moskovits, Nano Lett. **11**, 5548 (2011).